

Computational Models of Defect Clustering for Tethered Bilayer Membranes

Tomas Raila[1(✉)], Marija Jankunec[2], Tadas Meškauskas[1], and Gintaras Valinčius[2]

[1] Institute of Computer Science, Vilnius University, Vilnius, Lithuania
tomas.raila@mif.vu.lt
[2] Life Sciences Center, Vilnius University, Vilnius, Lithuania

Abstract. This study deals with computational modeling of defect clustering effects observed in bilayer phospholipid membranes. Two defect clustering models (algorithms) are presented and compared with the random defect distribution approach. Specific defect distribution instances are evaluated using a simple methodology based on Voronoi diagrams and statistical properties of their sector areas. Computational experiments are performed by using the models to generate synthetic defect distributions with different parameter combinations. The proposed methodology is also validated against atomic force microscopy images of real membranes with defects.

Keywords: Voronoi diagrams · 2D point clustering · Computer simulation · Phospholipid membranes

1 Introduction

Tethered bilayer phospholipid membranes (tBLMs) are popular models of biological membranes and versatile biosensing platforms, enabling studies of protein-membrane and similar interactions in a controlled way. In ideal conditions, such bilayers attached to conductive surface should exhibit dielectric properties. However, this is not the case in real situations due to membrane defects appearing either naturally or being introduced by various pore-forming chemical compounds [1]. One of experimental techniques used to assess electrical properties of such defected membranes is electrochemical impedance spectroscopy (EIS) [9]. This approach has traditionally been used to probe basic macroscopic properties of bilayers, in contrast of microscopy techniques (such as atomic force microscopy - AFM), which can provide extensive visual and structural information. Some recent studies showed that by modeling EIS spectra analytically [8] or numerically [3], certain structural properties of membranes can also be estimated.

One particular study in this specific topic dealt with synthetic EIS spectra computed for 3D membrane models using finite-element analysis (FEA) [6,7].

© Springer Nature Switzerland AG 2020
O. Gervasi et al. (Eds.): ICCSA 2020, LNCS 12253, pp. 496–504, 2020.
https://doi.org/10.1007/978-3-030-58814-4_35

EIS spectral features were used to estimate basic properties of membrane defects, such as their size and density. Results indicated qualitative similarities of EIS response between regular and random defect distributions. Modeled EIS spectra and synthetic defect distributions were also compared to experimentally obtained AFM and EIS data, indicating a good fit in most situations. However, it was found that defect clusters cause inconsistencies between EIS spectra computed for synthetic and experimental defect distributions, preventing the proposed methodology from being applicable in such cases. This study goes further into the defect clustering phenomenon. We present two parameterized defect clustering models which are used to generate synthetic clustered defect distributions. They are numerically evaluated by applying a simple methodology based on Voronoi diagrams and their basic statistical properties. The main objective is to determine if the described models can be used to qualitatively differentiate clustered and random defect distributions. Another investigated question is whether the proposed methodology has the potential to be further developed to enable quantitative evaluation of defect clustering effects in tBLM membranes based on experimental AFM or EIS data. In addition to computational experiments carried out with synthetic data we also validate the methodology by using real defect distributions experimentally registered with AFM.

2 Defect Distribution Models

The basic defect distribution type, used in the current and previous [7] study is the random defect distribution (Fig. 1), in which defect center coordinates (X and Y) are sampled from uniform probability distribution, independently for each defect. Due to its simplicity, this model is used as the baseline against which two more complex defect clustering models are assessed. In order to numerically express the properties of any defect distribution case, we use Voronoi diagrams [5]. The statistical distributions of sector areas obtained from computing such diagrams are characterized in terms of four summary statistics: standard deviation (σ), skewness, kurtosis and median absolute deviation (MAD). All studied defect distributions are bounded by hexagonal shape of the modeling domain in the same way as the membrane models solved with FEA technique in earlier work [7].

2.1 Attraction Model

This method is based on the assumption that defects naturally attract each other and thus tend to cluster together. Such type of object interaction is fundamental and common in nature (i.e. gravitational and electromagnetic forces) and also applicable in biological membrane models [4]. In this model attraction takes effect if the distance between two defects is below the predefined threshold d_T, which can be expressed in one of two ways:

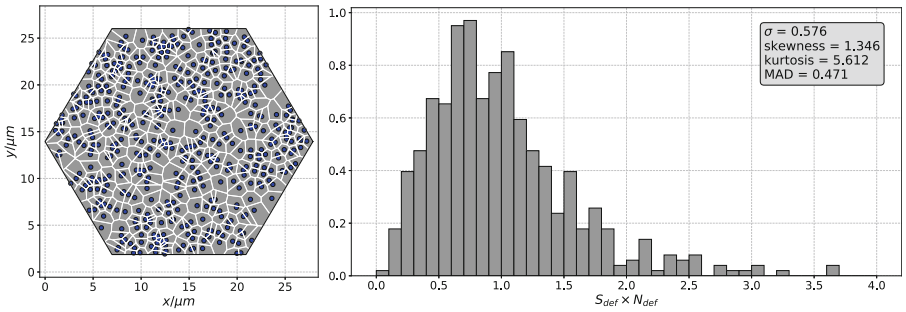

Fig. 1. Example of random defect distribution. Left: Voronoi diagram of defects in the modeling domain. Right: histogram of Voronoi sector areas (normalized with respect to defect density) and their statistics.

– Number of defect radiuses (of the attracting defect).
– Fixed distance in nanometers.

Generating a clustered defect distribution involves the following steps:

1. Coordinates of the first defect are picked randomly from uniform distribution.
2. For each of the subsequent defects:
   (a) Initial coordinates for the current defect with radius r_c are selected randomly from uniform distribution
   (b) Closest existing defect is selected and designated as the attractor with radius r_a.
   (c) Distance between the current and attractor defects is calculated.
   (d) If the distance is below the predefined threshold d_T and above the minimum distance $1.5 * (r_c + r_a)$, the current defect is shifted towards the attractor defect. Minimum distance is retained to avoid defect overlapping.
   (e) Otherwise, if the distance is below the minimum distance of $1.5*(r_c+r_a)$, the current defect is shifted away from the attractor defect until distance between their centers matches the minimum distance.
   (f) If the updated coordinates of the current defect fall outside the hexagon area, the defect is discarded.

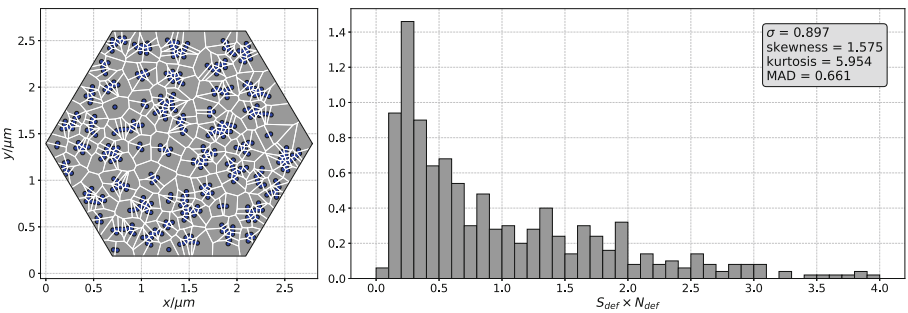

Fig. 2. Example of synthetic defect distribution generated using attraction model, where $d_T = 15$ (expressed in defect radiuses).

Figure 2 shows one example of synthetic clustered defect distribution, obtained by the described model. Distribution consists of 500 defects with equal radius (13 nm), dispersed with density of 100 defects per square micrometer. Such cases are characterized by tightly packed defect groups all containing a similar number of defects. This is reflected in the sector area histogram where the clustered defects represent a large number of small Voronoi sectors, in contrast with random distributions (Fig. 1).

2.2 LCN Model

This model is inspired by an idea that membrane defect clusters tend to form complex structures of varying size and shape, visually resembling clouds. This concept is relevant in computer graphics were various algorithms are used to procedurally generate cloud or smoke textures. For the implementation of this model we chose *lattice convolutional noise* (LCN) algorithm [2] and extended it by introducing two additional parameters by which the clustering effects are adjusted:

- Average relative cluster size: S
- Minimal probability of defect appearance: P

Parameter S is a positive real number which adjusts the scaling of LCN-generated initial image - smaller values correspond to a larger amount of small clusters. P is selected from $[0, 1]$ interval and represents the lower bound of probability field values. Defect distribution generation consists of the following steps:

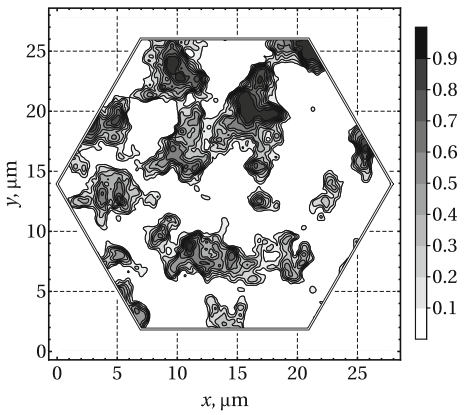

Fig. 3. Example of probability field generated with LCN algorithm.

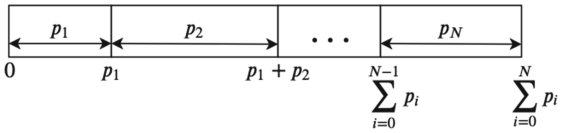

Fig. 4. Weighted roulette wheel selection of probability field pixels

1. By using the LCN algorithm a probability field of fixed resolution (i.e. 4096×4096) is generated and clipped by the hexagonal model domain shape (Fig. 3). Each pixel in the field corresponds to the probability p_i of defect appearing in that point.
2. Probability sum S_N is calculated for the field consisting of N points. Interval $[0; S_N]$ is divided into N subintervals, where each corresponds to probability p_i of respective pixel (Fig. 4).
3. For each defect a random number is uniformly sampled from interval $[0; S_N]$ and corresponding pixel of probability field is designated as the center of that defect.

This model produces clustered defect distributions (Fig. 5) which are visually distinct from the ones obtained by applying the attraction model (Fig. 2). Clusters exhibit different sizes and various irregularities which also reflected by statistical properties of Voronoi sector areas, where the majority of small sectors are offset by a number of very large ones.

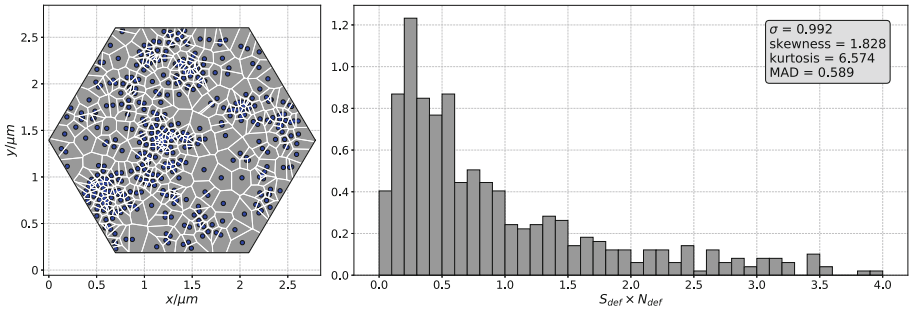

Fig. 5. Example of synthetic defect distribution generated using LCN model, where $S = 1$ and $P = 0.1$.

3 Experiments

3.1 Synthetic Data

In order to differentiate random and clustered defect distributions using a simple statistical approach, a number of synthetic defect distributions were generated by applying the proposed models with different parameter combinations

(Table 1). A total of 54 and 48 combinations for attraction and LCN models respectively were examined and summary statistics were computed for 100 independently generated cases for each option. In the same way, statistical properties of random defect distributions were determined from 100 independently generated cases. Each defect distribution consisted of 500 defects. Defect densities and sizes for attraction model were selected by likely scenarios examined in the earlier study [7]. Other values were chosen arbitrarily, to cover a wide range of visually different clustering cases. Sector areas in all cases were normalized with respect to defect density.

Table 1. Clustering model parameter values used in synthetic defect distribution generation.

Model type	Model parameter	Values
Attraction model	Defect density N_{def}	1; 10; 100
	Defect size R_{def} (nm)	0.5; 13; 25.5
	Attraction threshold[1] d_T	5; 10; 15; 20; 25; 30
LCN model	Min. probability P	0; 0.03; 0.06; 0.09; 0.12; 0.15
	Cluster size S	0.25; 0.5; 0.75; 1; 1.25; 1.5; 1.75; 2

[1] Expressed as the number of defect radiuses (R_{def}).

Standard deviation was chosen for the purpose of comparing clustered and random distributions. The baseline $\sigma = 0.54$ was found to be the average case for random defect distribution model, as determined from 100 independently generated instances. Attraction model results (Fig. 6) show very different σ trends for various defect size (R_{def}) and density (N_{def}) values. In case of small (0.5 nm) defects it is impossible to distinguish the clustered and random distributions. Similar issue applies for medium size (13 nm) defects with low density, although density increase introduces clear trend of σ growth depending on attraction threshold. Interesting effect of largest σ growth with medium defect density can be observed in largest (25 nm) defect case.

Figure 7 illustrates the dependency of standard deviation values by S and P parameters of LCN model. By decreasing the values of both parameters, standard deviation approaches the random distribution baseline, but does not cross that threshold. Although a clear increasing trend can be observed in all P cases, the specific clustering parameter values for a given clustered distribution cannot be unambiguously estimated just from the standard deviation of its Voronoi sector areas.

3.2 AFM Data

To validate the proposed methodology against real-world data, three AFM images of tBLMs affected with pore-forming toxin vaginolysin (VLY) were obtained. Each image covers membrane area of $6\,\mu\text{m} \times 6\,\mu\text{m}$, captured at

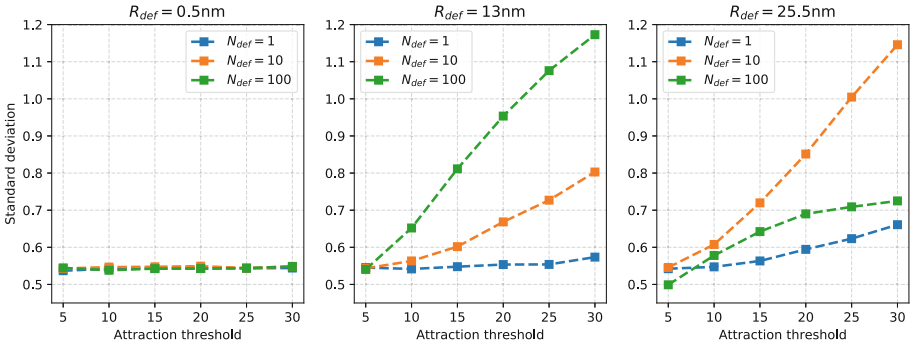

Fig. 6. Standard deviation values of Voronoi sector areas of generated synthetic defect distributions using attraction model.

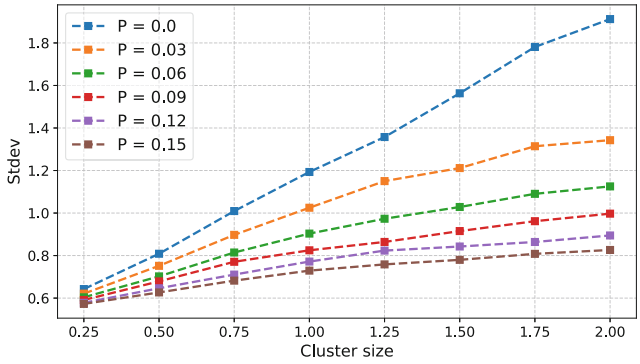

Fig. 7. Standard deviation values of Voronoi sector areas of generated synthetic defect distributions using LCN model with different parameter values.

1536×1536 resolution. Figure 8 illustrates one such example with Voronoi diagram overlaid on top of AFM image where several defect clusters, characterized by a large number of small sectors, can be observed. Coordinates of the defects present in each image were annotated manually by domain expert and Voronoi diagrams with corresponding statistical properties were computed for all cases (Table 2). Results show that experimentally registered defect distributions are significantly different from baseline random case in terms of standard deviation and MAD, although this does not apply for skewness and kurtosis.

Based on synthetic clustered distribution properties (Fig. 6 and 7) and baseline values of random distribution model, all three AFM-registered defect distributions can be classified as being clustered and distinct from random cases. However, unambiguously determining the more suitable clustering model and its parameters is not possible. Both attraction and LCN models can produce distributions with matching σ values, however, the attraction model depends more on the overall features of real defect distribution (defect size and density), which

might be difficult to estimate or measure experimentally. As noted in earlier work [7], radiuses of membrane defects (introduced by VLY) usually fall in range from 13 nm to 25 nm. This fact might be useful in estimating attraction model parameters based on summary statistics (σ and others). On the other hand, the LCN algorithm does not depend on defect size and density parameters and can be considered as more versatile.

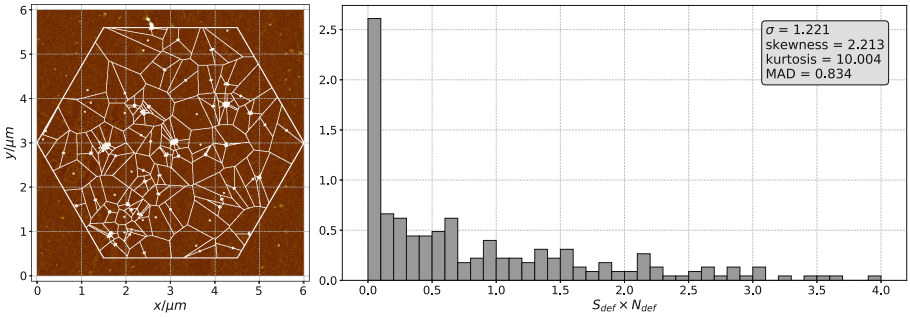

Fig. 8. Example of clustered defect distribution obtained from an AFM image of a real tBLM membrane sample.

Table 2. Statistical properties of Voronoi sector areas of experimentally registered defect distributions in comparison with random defect distribution properties.

Case ID	N	N_{def}	Stdev	Skewness	Kurtosis	MAD
AFM #1	234	10.01	1.22	2.21	10.00	0.83
AFM #2	148	6.33	1.12	1.80	6.52	0.70
AFM #3	235	10.05	0.88	1.21	4.25	0.79
Random	–	–	0.54	1.18	5.38	0.49

4 Results and Conclusions

In this work we presented two defect clustering algorithms and a simple methodology for evaluating clustering effects, based on Voronoi diagrams and statistical properties of their sector areas. Experiments with synthetic clustered defect distributions showed different σ and other property trends depending on model parameter combinations. LCN model was considered to be more versatile in differentiating the random and clustered defect distributions, although the results are only qualitative and the current approach is not yet applicable in deriving clustering parameters for a given specific defect distribution case. The usefulness of attraction model for this task also cannot be ruled out, although its applicability depends on defect size and density properties. Standard deviation of Voronoi sector areas proved to be useful in distinguishing between clustered

and randomly-distributed defect cases. Although the small amount of available AFM data prevents the statistically-proven conclusions to be made, analysis tentatively proved the usefulness of the proposed methodology in evaluating the clustering effects in real tBLM membranes.

Next steps in this research direction would involve a more thorough statistical analysis with the larger amount of AFM data, further clustering model development and application of the methodology on experimental EIS data.

References

1. Cornell, B.A., et al.: A biosensor that uses ion-channel switches. Nature **387**, 580–583 (1997)
2. Ebert, D., et al.: Texturing and Modeling: A Procedural Approach, 3rd edn., December 2002
3. Kwak, K.J., et al.: Formation and finite element analysis of tethered bilayer lipid structures. Langmuir **26**, 18199–18208 (2010)
4. Mugler, A., Bailey, A., Takahashi, K., Wolde, P.: Membrane clustering and the role of rebinding in biochemical signaling. Biophys. J. **102**, 1069–1078 (2012). https://doi.org/10.1016/j.bpj.2012.02.005
5. Okabe, A., Boots, B., Sugihara, K., Chiu, S.: Spatial Tessellations: Concepts and Applications of Voronoi Diagrams, vol. 43, January 2000. https://doi.org/10.2307/2687299
6. Raila, T., Meškauskas, T., Valinčius, G., Jankunec, M., Penkauskas, T.: Computer modeling of electrochemical impedance spectra for defected phospholipid membranes: finite element analysis. In: Sergeyev, Y.D., Kvasov, D.E. (eds.) NUMTA 2019. LNCS, vol. 11974, pp. 462–469. Springer, Cham (2020). https://doi.org/10.1007/978-3-030-40616-5_44
7. Raila, T., Penkauskas, T., Jankunec, M., Dreižas, G., Meškauskas, T., Valinčius, G.: Electrochemical impedance of randomly distributed defects in tethered phospholipid bilayers: Finite element analysis. Electrochim. Acta **299**, 863–874 (2019)
8. Valinčius, G., Meškauskas, T., Ivanauskas, F.: Electrochemical impedance spectroscopy of tethered bilayer membranes. Langmuir **28**, 977–990 (2012)
9. Valinčius, G., Mickevičius, M.: Tethered phospholipid bilayer membranes: an interpretation of the electrochemical impedance response. In: Iglič, A., Kulkarni, C.V., Rappolt, M. (eds.) Advances in Planar Lipid Bilayers and Liposomes, vol. 21, pp. 27–61. Academic Press (2015). (Chap. 2)